

## Total oxidation of toluene over calcined trimetallic hydrotalcites type catalysts

Luz A. Palacio<sup>a,b</sup>, Juliana Velásquez<sup>b</sup>, Adriana Echavarría<sup>b</sup>, Arnaldo Faro<sup>c</sup>,  
F. Ramôa Ribeiro<sup>a</sup>, M. Filipa Ribeiro<sup>a,\*</sup>

<sup>a</sup> Instituto Superior Técnico, IBB - Centro de Engenharia Biológica e Química, Universidade Tecnica de Lisboa, Av. Rovisco Pais, 1049-001 Lisboa, Portugal

<sup>b</sup> Grupo Catalizadores y Adsorbentes, Universidad de Antioquia 1-317, A.A. 1226 Medellín, Colombia

<sup>c</sup> Departamento de Fisicoquímica, Instituto de Química, Universidade Federal do Rio de Janeiro, Ilha do Fundão, CT bloco A, Rio de Janeiro, Brazil

### ARTICLE INFO

#### Article history:

Received 4 June 2009

Received in revised form 7 December 2009

Accepted 8 December 2009

Available online 16 December 2009

#### Keywords:

Hydrotalcite  
Toluene  
Combustion  
VOCs

### ABSTRACT

Two trimetallic ZnCuAl and MnCuAl hydrotalcites have been successfully synthesized by a co-precipitation method. The manganese based material was identified as a new hydrotalcite phase. Both lamellar precursors were calcined at 450 and 600 °C and the resulting catalysts were tested on reaction of total oxidation of toluene. The solids were characterized by X-ray diffraction, thermal analysis, atomic absorption spectroscopy, Fourier transformed infrared spectroscopy, N<sub>2</sub> adsorption and H<sub>2</sub> temperature-programmed reduction.

It was found that ZnCuAl materials are composed of copper and zinc oxides supported on alumina; while MnCuAl ones comprise basically spinel phases, which were not completely identified. The catalytic behavior of the calcined samples showed that Mn hydrotalcite calcined at 450 °C exhibited the best catalytic performance that corresponds to 100% toluene conversion into CO<sub>2</sub> at about 300 °C.

© 2010 Elsevier B.V. All rights reserved.

### 1. Introduction

The layered double hydroxides (LDHs) or hydrotalcite-like materials have been widely investigated owing to their potential applications as ion exchangers, adsorbents, ionic conductors, catalysts and catalyst precursors, supports, pharmaceuticals and so on [1]. The general chemical formula of these lamellar solids can be written as  $[M_{1-x}^{2+}M_x^{3+}(\text{OH})_2](A^{n-})_{x/n} \cdot m\text{H}_2\text{O}$  where M<sup>2+</sup> and M<sup>3+</sup> are divalent and trivalent cations (Mg<sup>2+</sup> and Al<sup>3+</sup> in the natural hydrotalcite) that occupy the center of M(OH)<sub>6</sub> octahedral units and A<sup>n-</sup> is a compensation anion [2].

A large number of LDHs with a wide variety of M(II)–M(III) cation pairs, as well as different anions in the interlayer have been reported in the scientific literature as stated in reviews like those from Sels et al. and Crepaldi et al. [3,4]. However, LDHs totally replacing the Mg<sup>2+</sup> for transition metals in the brucite-like layer are scarce due to the difficulty in obtaining a pure hydrotalcite phase. An outstanding factor that increases the effort for the synthesis of these materials is that thermal decomposition of LDHs precursors leads to the formation of M<sup>2+</sup> and M<sup>3+</sup> mixed oxides exhibiting fine dispersion of metal cations and high surface area, compared with those obtained from direct methods; besides memory effect, good thermal stability and good mixed oxides homogeneity are other properties of this type of materials [5].

The mixed oxides obtained from hydrotalcites have shown a very good performance in many reactions of industrial interest like CH<sub>4</sub> and methanol reforming [6,7], hydrodesulfurization of gasoline [8], removal of SO<sub>2</sub> and NO<sub>x</sub> [9] and also for catalytic combustion of VOCs [10–12].

Volatile organic compounds (VOCs) are dangerous air pollutants that can be converted by catalytic combustion, which represents a very promising alternative for their elimination, due to the energy saving that it can provide comparatively to thermal combustion and also because transition metal based oxides can replace traditional noble metal based catalysts, because of their low cost and stability [13].

Recently, some hydrotalcites have been reported as precursors for obtaining catalysts for VOCs elimination, mainly toluene. They exhibit promising results, but combustion temperatures are not lower than those observed with noble metal catalysts. The tested hydrotalcites are based on the systems Cu–Mg–Al [10], Co–Mn–Al [14], Mg–Mn–Al [12], Cu(Zn)–Mn(Al) [15] for toluene combustion and Ni–Al for toluene and ethanol combustion [16].

In this work, hydrotalcite-like materials have been used as catalyst precursors, and their catalytic behavior was evaluated in toluene combustion. MnCuAl and ZnCuAl trimetallic hydrotalcites were synthesized and calcined. The first one evidences a new composition with hydrotalcite structure that differs from the one reported by Zimowska et al. [15] in terms of composition of the LDH and structure of the calcined material. Toluene was selected as VOC model molecule because it is a commonly used solvent in

\* Corresponding author. Tel.: +351 21 841 78 72; fax: +351 21 841 91 98.

E-mail address: [filipa.ribeiro@ist.utl.pt](mailto:filipa.ribeiro@ist.utl.pt) (M.F. Ribeiro).

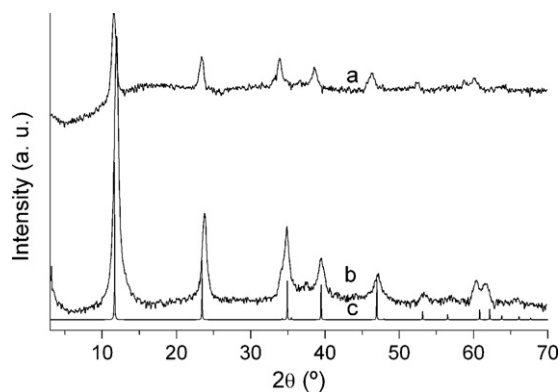


**Fig. 1.** XRD patterns for the precursors. (a) MnCuAl, (b) ZnCuAl and (c) calculated MgAl hydrotalcite pattern.

chemical and processing industries and controlling its emission in the atmosphere is becoming relevant [17].

The precursor and the catalysts were characterized by powder X-ray diffraction (XRD), atomic absorption spectroscopy (AAS), thermal analysis (TG/DTA), Fourier transformed infrared spectroscopy (FTIR),  $N_2$  adsorption and hydrogen temperature-programmed reduction ( $H_2$ -TPR).

## 2. Experimental

### 2.1. Catalysts preparation

The precursors, MnCuAl and ZnCuAl hydrotalcite-type materials were obtained by a co-precipitation method. Two solutions were prepared, the first one containing the metal sources (nitrates for the ZnCuAl and sulfates for MnCuAl) with Zn/Al ratio equal to 3 and Mn/Al ratio equal to 6. Separately, a second solution containing NaOH (4.2 M) and an excess of  $Na_2CO_3$  was prepared and then added dropwise to the first solution until a final pH of 10, under vigorous stirring. The resulting slurry (with a molar ratio of 3/3/1 for MnCuAl and 1.5/1.5/1 for ZnCuAl) was subsequently aged for 24 h at room temperature. Then the precipitate was filtered and rinsed with deionized water until to reach neutral pH. The resulting solid was dried at 50 °C and a LDH material was finally achieved.

The catalysts were obtained by calcination of the precursor at 450 and 600 °C, under static air and with a heating rate of 10 °C  $min^{-1}$ .

### 2.2. Catalysts characterization

Powder XRD patterns were obtained in a Rigaku Miniflex diffractometer using Cu K $\alpha$  radiation, operated at 40 kV, 30 mA and 2°  $min^{-1}$ . The phases were identified using databases PDF-2 (Powder Diffraction File) and ICSD (Inorganic Crystal Structure Database). The precursor was analyzed by thermogravimetry in a TA Instruments Hi-Res TGA 2950 under a nitrogen flow of 30 mL  $min^{-1}$  and 10 °C  $min^{-1}$  heating rate up to 800 °C. The differential thermal analysis was carried out in a TA Instruments 1600 DTA under the same conditions. The metal content analysis was carried out in a Solaar Unicam equipment. The  $N_2$  adsorption-desorption isotherms were obtained on a Micromeritics ASAP 2010 instrument after outgassing the samples at 150–200 °C. The surface area was calculated using the BET equation from  $N_2$  adsorption isotherms. Infrared spectra of the samples diluted to 1 wt.% in KBr were obtained in a PerkinElmer Spectrum One equipment. Temperature-programmed reduction with hydrogen was carried out in a Autochem II Micromeritics equipment. The catalysts were heated under argon flow (30 mL  $min^{-1}$ ) at 300 °C for

30 min and then cooled down to room temperature; then, reduction of the catalysts was performed under  $H_2$  (5 vol.%) / Ar flow (30 mL  $min^{-1}$ ) and heating at 10 °C  $min^{-1}$  from room temperature to 1000 °C.

### 2.3. Catalytic tests

Toluene oxidation was carried out at atmospheric pressure in a fixed bed reactor, using 200 mg of catalyst. The reactant gas mixture, air containing toluene (800 ppm), was prepared by passing air through a saturator containing toluene, which was kept at –3 °C. The reaction mixture was fed at a flow rate of 15 L  $h^{-1}$  (75 L  $h^{-1} g^{-1}$ ), the catalyst was in powder form, and with a size distribution in which 90% was lower than 0.841 mm. The reaction was carried out under temperature-programmed condition (TPSR), from 100 °C up to 450 or 600 °C (catalyst calcination temperature) with a heating rate of 3 °C  $min^{-1}$ . The feed and the reaction products were analyzed by on-line gas chromatography (HP 5890 gas chromatograph equipped with a Poraplot Q column) for hydrocarbons and IR Siemens Ultramat 23 analyzer for  $CO_2$  and CO. Before the reaction, the catalysts were pretreated under a 15 L  $h^{-1}$  air flow at 450 or 600 °C for 1 h. The catalytic activity was evaluated in terms of conversion to  $CO_2$  by measuring its concentration each 2 min.

## 3. Results and discussion

### 3.1. X-ray diffraction

The formation of hydrotalcite phases was confirmed from the XRD patterns of the precursors (see Fig. 1). The appearance of a single crystalline phase can be observed for both materials. The experimental patterns are compared with those calculated for MgAl hydrotalcite taken from PDF (PDF:89-460).

Fig. 2 shows that the collapse of the LDH structure due to calcinations and the formation of oxides with low crystallinity can occur. When ZnCuAl is calcined at 450 °C, an amorphous phase is obtained but, when it is calcined at 600 °C the individual divalent metal oxides are obtained (ZnO PDF:36-1451 ICSD:26170, CuO PDF:45-937 ICSD: 69758). The absence of aluminum oxide compounds is due to its transformation into an amorphous phase that acts as support for the other oxides.

In the case of MnCuAl samples, the calcination (at 450 and 600 °C) leads to the formation of a spinel phase, which occurred at a relatively low temperature in comparison to the ones normally necessary for the formation of these materials (>800 °C) [5]. Nevertheless, the sample calcined at 450 °C showed lower crystallinity than the sample calcined at 600 °C. Several compositions in spinel phase were found in the databases with the same elements than those present in our samples and with similar XRD patterns (CuMn $_2$ O $_4$  PDF:74-2422 ICSD: 30078, CuAl $_2$ O $_4$  PDF:76-2295, Mn $_2$ AlO $_4$  PDF:29-881, MnAl $_2$ O $_4$  PDF:21-880, CuAlMnO $_4$  PDF:43-285).

Based only on XRD data, it is impossible to identify which of these phases are present in the calcined MnCuAl samples or if there is a mixture of them. Nevertheless, from the slight differences between the XRD patterns spinel phases, CuMn $_2$ O $_4$  and MnAl $_2$ O $_4$ , provided the best fitting. In Fig. 2, only the pattern for the CuMn $_2$ O $_4$  phase is shown because the one for MnAl $_2$ O $_4$  is almost the same. However, by the high possibility of Mn in the precursor be mainly in state oxidation of 3+, the hypothesis that the spinel formed be CuMn $_2$ O $_4$  is very possible.

### 3.2. Thermal analysis

TG/DTA profiles from Figs. 3 and 4 show a first peak at about 150 °C, assigned to the removal of interlayer water molecules. The

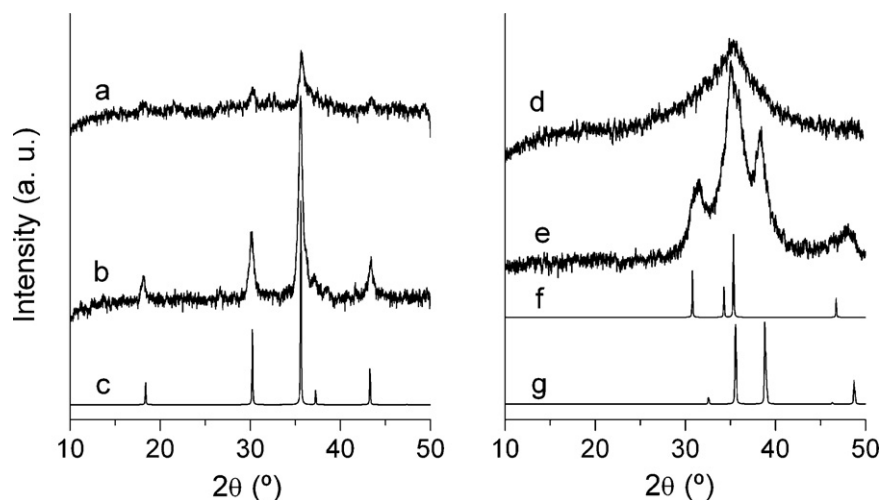


**Fig. 2.** XRD patterns for the calcined precursors. (a) MnCuAl450, (b) MnCuAl600, (c)  $\text{CuMn}_2\text{O}_4$  spinel calculated pattern, (d) ZnCuAl450, (e) ZnCuAl600, (f) ZnO calculated pattern and (g) CuO calculated pattern.

subsequent steps correspond to weight losses due to the decomposition of interlayer anions and dehydroxylation of the hydroxide layers. This last occurrence evidenced by a broad band, not clearly defined in the DTA curves, seems to be a special feature for Cu containing hydrotalcites [4,18]. This phenomenon can be explained by the distortion that this cation introduces into the structure (Jahn-Teller effect), leading to start the decomposition at lower temperatures (compared with MgAl hydrotalcite [5]). Simultaneously, part of the carbonates is retained up to temperatures around  $600^\circ\text{C}$ , seeming that Cu is responsible for the stabilization of carbonate anions. Even though, the layered crystal structure

collapses at lower temperatures, the weight loss continues until to  $600^\circ\text{C}$ , reaching more than 20% (26% for ZnCuAl and 23% for MnCuAl).

This characteristic behavior of Cu hydrotalcites has been described in the literature from identification of the gases evolved during the thermal decomposition process continuously monitored with a mass spectrometer [19,20].

In Fig. 4 the DTA curve evidences an exothermic peak in the temperature range  $500\text{--}600^\circ\text{C}$ , which in Ni–Mn hydrotalcites [21], has been assigned to oxidation reactions of Mn(III) into Mn(IV). In our case, the exothermic peak can be associated with oxidation of remaining Mn(II) into Mn(III). Several reports concerning to the synthesis of containing Mn hydrotalcites have found that Mn(II), as initially is in the source metal (in our case, manganese sulfate), is almost completely oxidized to Mn(III) in the co-precipitation process, when it is carried out in air [12,15,21,22].

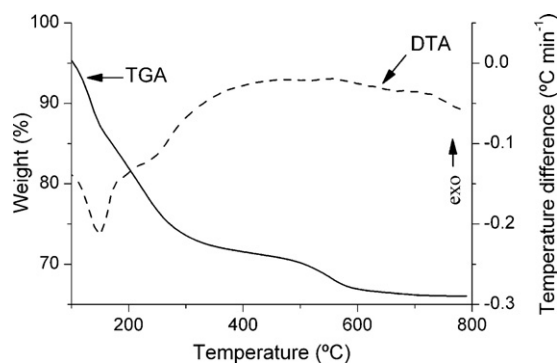


**Fig. 3.** Thermal decomposition for the ZnCuAl hydrotalcite-like precursors.

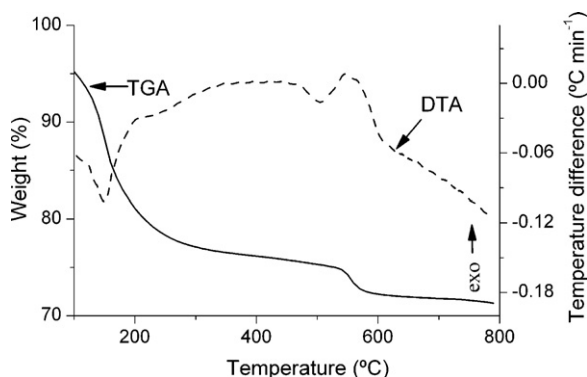


**Fig. 4.** Thermal decomposition for the MnCuAl hydrotalcite-like precursors.

### 3.3. Elemental analysis

The metal contents of prepared hydrotalcites are shown in Table 1. The atomic ratio in the reaction mixture for the ZnCuAl material is higher than the expected one (1.5/1.5/1), showing that aluminum species in solution were not totally transferred to the solid. In the case of MnCuAl, the atomic ratio (3/3/1) in the reaction mixture is much higher than in the solid, indicating that part of Mn and Cu was kept in solution rather than incorporated into the solid and, in contrast with ZnCuAl samples that evidence a greater incorporation of transition metals in the solid. The differences in metal contents can be ascribed to preferential precipitation due the variable pH, concentration and supersaturation levels involved in this synthesis method.

### 3.4. Nitrogen adsorption

Table 2 presents the BET surface areas of the mixed oxides produced by calcination of the hydrotalcite-like precursors. The materials calcined at  $600^\circ\text{C}$  present a smaller surface area due to sintering of the particles or formation of more crystalline products, but this decrease is lower for ZnCuAl sample. After calcination at  $450^\circ\text{C}$  the MnCuAl sample shows a high surface area compared with the same oxides synthesized by a direct method [23]. The adsorption isotherms are very similar and a representative one was plotted in Fig. 5. They are typical of non-porous materials with nitrogen condensation at high relative pressures, meaning that the

**Table 1**  
Elemental analysis of the hydrotalcite-like materials.

Sample	Zn or Mn (%)	Cu (%)	Al (%)	(Cu + (Zn or Mn))/Al <sup>a</sup>	Cu/Al <sup>a</sup>	TGA weight loss (%) <sup>c</sup>
ZnCuAl	22.2	21.4	4.2	4.3 (3) <sup>b</sup>	2.2 (1.5) <sup>b</sup>	26
MnCuAl	19.0	17.6	6.4	2.6 (6) <sup>b</sup>	1.1 (3) <sup>b</sup>	23

<sup>a</sup> Atomic ratio.

<sup>b</sup> The values between parentheses correspond to the atomic ratio in the reaction mixture.

<sup>c</sup> It was measured between 100 and 600 °C.

main part of the surface area presented in the Table 2 is due to the external surface area of small particles.

### 3.5. Infrared spectroscopy analysis

The results of FTIR analysis for the precursors and calcined samples are shown in Figs. 6 and 7. In spectra of the uncalcined samples, the normal vibrations of hydrotalcite are observed. The broadest and most intense (around 3400 cm<sup>-1</sup>) band corresponds to OH stretching mode (structural hydroxyl groups, water molecules in the interlayer zone, physisorbed and free water). The band around

**Table 2**  
BET surface areas of calcined hydrotalcites.

Catalyst	S <sub>BET</sub> (m <sup>2</sup> g <sup>-1</sup> )
ZnCuAl450	80
ZnCuAl600	65
MnCuAl450	108
MnCuAl600	45

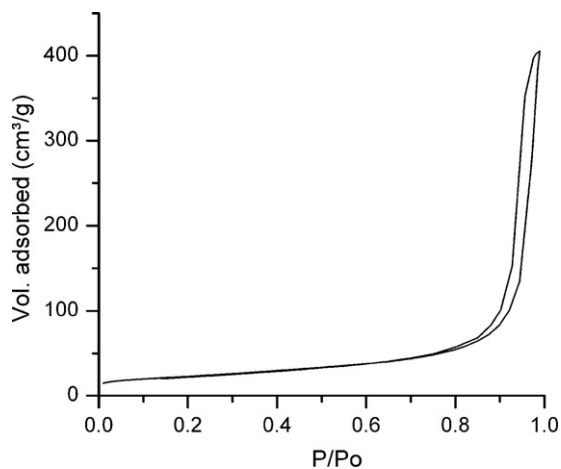


Fig. 5. Nitrogen adsorption isotherm of calcined hydrotalcite ZnCuAl450.

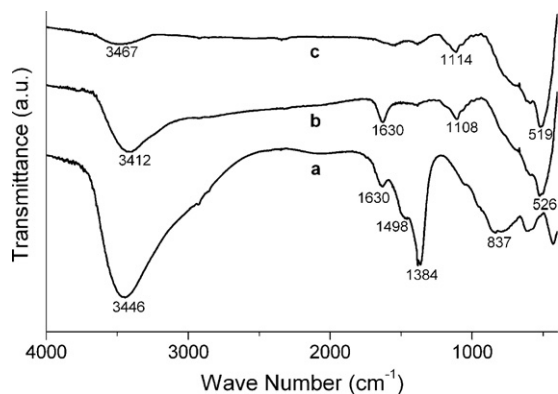


Fig. 6. Infrared spectra of ZnCuAl precursor (a) and calcined samples (b: at 450 and c: at 600 °C).

1600 cm<sup>-1</sup> is attributed to water HOH bending vibration (angular deformation) [24]. The carbonate bands are observed around 800 cm<sup>-1</sup> (out of plane bending,  $\nu_2$  mode) and 1300 cm<sup>-1</sup> (asymmetric stretching,  $\nu_3$  mode) while the vibration at ca. 1500 cm<sup>-1</sup> corresponds to a symmetry reduction of the carbonate anions owing to the interaction with metal cations with just one of their oxygen atoms [25]. The bands at about 1100 cm<sup>-1</sup> are associated with O–H deformations [20].

The bands lower than 600 cm<sup>-1</sup> are attributed to M–O interaction (M = Al, Zn, Cu, Mn) [26], but a strict assignment of the bands is difficult because of the complex band profile and the overlap of the bands when more than one metal is present. In the case of ZnCuAl, the band that appears at 837 cm<sup>-1</sup> for the precursor is assigned to the symmetric stretching of CO<sub>2</sub>, but it disappears after calcination, and a new band arises at ca. 520 cm<sup>-1</sup>, corresponding to CuO formation [27]. Similar bands are observed in MnCuAl, but in this case the frequency at ca. 505 cm<sup>-1</sup> can be attributed to the copper vibration in spinel phase. It can be seen that in the structural region (1000–400 cm<sup>-1</sup>), ZnCuAl450 and ZnCuAl600 have similar spectra, indicating that the two samples have the same nature, namely the CuO–ZnO mixture, not observed in XRD for ZnCuAl450. In the calcined samples some of the carbonate and water bands are still present, confirming the discussion on thermal analysis. Clear differences are observed (region 1000–400 cm<sup>-1</sup>) between precursor and catalysts, showing the changes caused by the transformation of the lamellar structure to mixed oxides.

### 3.6. Hydrogen temperature-programmed reduction

Results of H<sub>2</sub> temperature-programmed reduction are shown in Fig. 8 and summarized in Table 3. Reduction peaks above 850 °C were not observed. All the samples present two reduction peaks, and the reduction of MnCuAl450 sample starts at the lowest temperature. The first reduction peak of all samples occurs at about 300 °C; this temperature has been reported in the literature for the reduction of Cu<sup>2+</sup> species to Cu<sup>+</sup> or Cu<sup>0</sup> [17]. In a study performed by other researchers [28–30], they observed the reduction behavior of Cu/ZnO catalysts with XANES measurements, and they

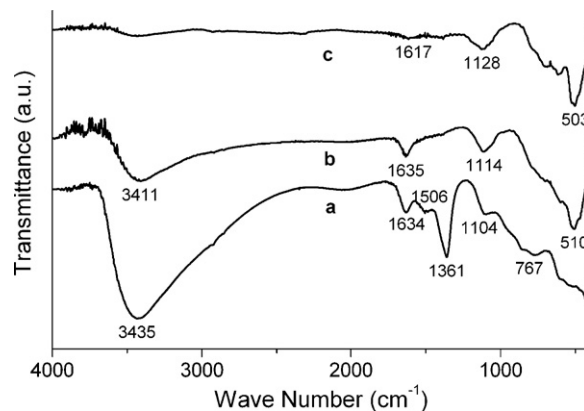
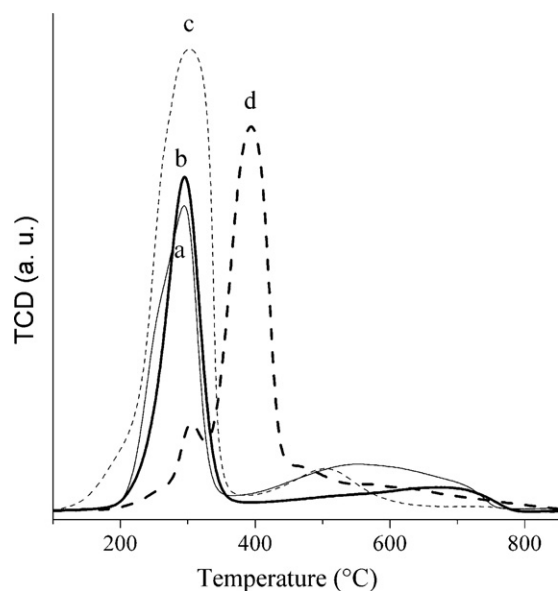


Fig. 7. Infrared spectra of MnCuAl precursor (a) and calcined samples (b: at 450 and c: at 600 °C).



**Fig. 8.** Hydrogen TPR profiles for the calcined HTs. Continuous line: ZnCuAl (a: calcined at 450 and b: calcined at 600) and dash line: MnCuAl (c: calcined at 450 and d: calcined at 600).

confirmed that up to 300 °C, the reduction process can be attributed to  $\text{Cu}^{2+} \rightarrow \text{Cu}^+ \rightarrow \text{Cu}^0$ .

On the other hand, Mn and Zn oxides are more difficult to reduce than Cu. In copper–manganese oxide catalysts, a reduction peak centered at 300 °C has been attributed to the reduction of  $\text{Mn}_2\text{O}_3$  to MnO and another one at around 405 °C is related to the reduction of  $\text{Mn}_5\text{O}_8$  to MnO [31]. Up to 1000 °C, no further reduction of  $\text{Mn}^{2+}$  was observed [23]. In other experiments performed with ZnO, partial reduction of zinc was observed, with a maximum at around 600 or 780 °C for two different samples, being the second one more crystalline than the first [32].

Taking into account this information, we assumed that in our calcined hydrotalcites the first evolution in the TPR profile is due to the copper reduction and the subsequent evolutions are due to the partial reduction of Zn or Mn. The materials containing Mn were more extensively reduced, as can be observed from the total  $\text{H}_2$  consumption shown in Table 3. The highest difference in reduction behavior was observed with MnCuAl600, which was reduced at temperature significantly higher than the other materials. This can be explained because this sample is a more crystalline phase with less surface defects in which hydrogen can be dissociated [19,31].

The theory indicates that for each  $\text{Cu}^{2+}$  fully reduced to  $\text{Cu}^0$ , a consumption of 1 mole of  $\text{H}_2$  is needed. From Table 3, the values corresponding to  $\mu\text{mole Cu/g catalyst}$  can be compared with total  $\mu\text{mole H}_2/\text{g catalyst}$ , and it can deduced that the first peak that appears in almost all samples (except in MnCuAl600) may be

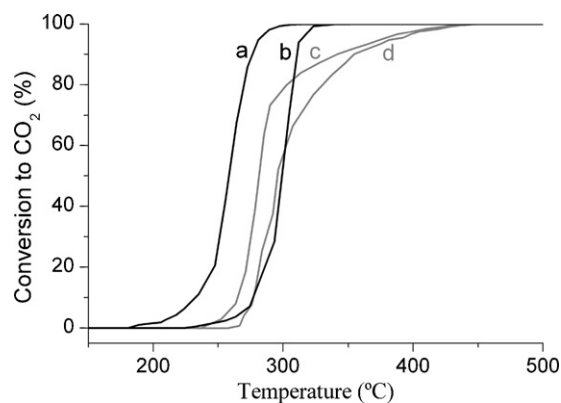
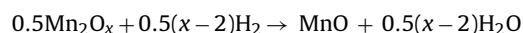


**Fig. 9.** Conversion of toluene into  $\text{CO}_2$  observed with the catalysts. (a) MnCuAl450, (b) MnCuAl600, (c) ZnCuAl600 and (d) ZnCuAl450 (800 ppm toluene in air,  $\text{GHSV} = 84750 \text{ h}^{-1}$ ).

attributed to the reduction of copper to the metallic state. In the MnCuAl450 the remaining of the first peak can be attributed to the initial reduction of Mn and in the ZnCuAl samples to experimental error. In the case of MnCuAl600, the first small peak is assigned to partial reduction of copper and the second one to completion of Cu reduction to metallic form and reduction of part of Mn ions.

In order to attempt to estimate the initial oxidation state of Mn in the catalysts, some calculations were made. The copper total reduction contribution (fourth column) was subtracted from the total  $\text{H}_2$  consumption (sixth column) as it is shown in the seventh column of Table 3 (remaining  $\text{H}_2$  uptake after Cu reduction in  $\mu\text{mol H}_2/\text{g catalyst}$ ). As mentioned before, the remaining consumption of  $\text{H}_2$  after complete copper reduction is assigned to manganese partial reduction. Then, the results of the seventh column were divided by the concentrations of Mn (fifth column) in order to obtain the values in the last column, expressed as  $\mu\text{mol H}_2/\mu\text{mol Mn}$ . As mentioned above, under our experimental conditions the maximum reduction that could be achieved for Mn would be to  $\text{Mn}^{2+}$ , as MnO. Taking into account the stoichiometry:



the initial oxidation state of Mn ( $x$ ) can be calculated from the  $\text{H}_2$  uptake per mol of Mn. Within the experimental error of TPR quantification,  $\text{H}_2:\text{Mn}$  ratios provide an average initial oxidation state of 3.2 for MnCuAl600 and 3.0 for MnCuAl450, which are in good agreement with the assumption that in the precursor almost all Mn is in oxidation state 3+. This is consistent with most of the Mn being part of a spinel phase in which Mn is the trivalent metal, such as  $\text{CuMn}_2\text{O}_4$ .

Similar calculations were did for  $\text{H}_2:\text{Zn}$  ratios, but in this case, the initial oxidation state was known and the TPR quantification was used to calculate the final average state oxidation of Zn, which

**Table 3**  
Summary of hydrogen temperature-programmed reduction.

Catalyst	Temperature (°C)		Metal concentration ( $\mu\text{mol metal/g catalyst}$ )		$\text{H}_2$ uptake ( $\mu\text{mol H}_2/\text{g catalyst}$ )		
	Onset	At maximum <sup>a</sup>	Cu	Mn or Zn	Total <sup>b</sup>	Remaining after Cu reduction <sup>b</sup>	Associated to Mn or Zn <sup>c</sup>
ZnCuAl450	140	294; 552	4.5	4.5	4.8; 2.6	0.3; 2.6	0.6
ZnCuAl600	140	295; 683	4.7	4.8	5.8; 1.0	1.1; 1.0 <sup>d</sup>	0.2
MnCuAl450	100	302; 506	3.5	7.5	7.0; 0.6	3.5; 0.6	0.5
MnCuAl600	170	302; 394	4.1	7.5	0.2; 8.2	0.0; 4.3	0.6

<sup>a</sup>The values separated by semicolon correspond to maximum temperature of each peak in TPR profile.

<sup>b</sup>The values separated by semicolon correspond to  $\text{H}_2$  uptake of peaks whose temperature maximum is in the third column.

<sup>c</sup>The units are  $\mu\text{mol H}_2/\mu\text{mol Mn or Zn}$ .

<sup>d</sup>Only the second value (1.0) is associated to Zn in the next column, for appearing at temperature higher than 600 °C.

**Table 4**  
Comparison of results observed in toluene catalytic combustion.

Catalyst	Toluene (g/m <sup>3</sup> )	S.V. (L h <sup>-1</sup> g <sup>-1</sup> )	T <sub>50</sub> (°C)	T <sub>100</sub> (°C)	Reference
NiAl	1	10	246–269	n.r. <sup>a</sup>	[16]
CuMn	0.2	–	–	–	[15]
CoMnAl	1800	30	247–287	250–350	[14]
CuMgAl	1	10	273–354	n.r. <sup>a</sup>	[10]
MnCuAl450	800 <sup>b</sup>	75	258	307	This work

<sup>a</sup> n.r.: not reached.

<sup>b</sup> ppm (mol).

was 0.8 for ZnCuAl450 and 1.6 for ZnCuAl600, confirming that the Zn is partially reduced.

### 3.7. Catalytic activity for toluene combustion

The catalytic results observed for toluene combustion are shown in Fig. 9. All catalysts present light-off temperatures  $T_{50}$  (50% conversion into CO<sub>2</sub>) below 300 °C. The total conversion of toluene into CO<sub>2</sub> (100% conversion) is more easily reached with the catalysts containing Mn than with Zn based catalysts. This can be due to the fact that the former have a larger amount of metal reducible species per mass of catalyst. The MnCuAl450 sample with best textural and reductive properties presented the highest activity ( $T_{50}$  = 258 °C and  $T_{100}$  = 297 °C). All catalysts are selective for CO<sub>2</sub>, because they do not produce any other oxidation products and only CO<sub>2</sub> was detected.

Copper catalysts are fairly active in the combustion of organic compounds [33,34]. Lately, also Mn containing catalysts have proved to be quite active for the destruction or combustion of toxic volatile organic compounds [11,15,35]. Fig. 9 shows that the differences in light-off temperatures are significant (ca. 50 °C); however, the differences in temperature of complete combustion were even higher (≥150 °C). In several cases reported in the literature 100% conversion was not even attained. Table 4 presents a comparison between MnCuAl450 sample (most active sample) and some results reported in other works that have used hydrotalcite-derived catalysts for toluene catalytic combustion.

Catalyst CuMn, which should be the most similar to our MnCuAl450 sample, showed very unusual results, since a CO<sub>2</sub> yield higher than 100% was reported for it and the experimental conditions were not well described, which excludes any comparison with our results. From the data reported in Table 4, it can be concluded that, despite the differences in operating conditions, the results observed with our catalyst are very attractive, especially if it is considered that catalytic tests were performed at a higher space velocity than in other works, and the light-off temperature is among the smallest ones reported.

## 4. Conclusion

Trimetallic hydrotalcites were successfully prepared with the co-precipitation method. MnCuAl hydrotalcite seems to be a new phase because no reference was found in XRD databases and in the literature. After calcination, both MnCuAl and ZnCuAl hydrotalcites produced active catalysts for toluene total combustion. The most active catalyst was obtained with MnCuAl hydrotalcite after calcination at 450 °C, which when compared to other hydrotalcite-derived materials reported in the literature, evidences very attractive light-off temperature.

## Acknowledgments

L.A. Palacio is grateful for a research grant from FCT (SFRH/BPD/20828/2004). Financial support for this work by the

Portuguese Foundation for Science and Technology (FCT) is gratefully acknowledged.

## References

- [1] F. Cavani, F. Trifirò, A. Vaccari, Hydrotalcite-type anionic clays: preparation, properties and applications, *Catal. Today* 11 (1991) 173–301.
- [2] A. Vaccari, Clays and catalysis: a promising future, *Appl. Clay Sci.* 14 (1999) 161–198.
- [3] B.F. Sels, D.E. De Vos, P.A. Jacobs, Hydrotalcite-like anionic clays in catalytic organic reactions, *Catal. Rev.—Sci. Eng.* 43 (2001) 443–488.
- [4] E.L. Crepaldi, J.B. Valim, Layered double hydroxides: structure, synthesis, properties and applications, *Quim. Nova* 21 (1998) 300–311.
- [5] R. Bastiani, I.V. Zonno, I.A.V. Santos, C.A. Henriques, J.F.L. Monteiro, Influence of thermal treatments on the basic and catalytic properties of Mg,Al-mixed oxides derived from hydrotalcites, *Braz. J. Chem. Eng.* 21 (2004) 193–202.
- [6] C.E. Daza, J. Gallego, J.A. Moreno, F. Mondragón, S. Moreno, R. Molina, CO<sub>2</sub> reforming of methane over Ni/Mg/Al/Ce mixed oxides, *Catal. Today* 133–135 (2008) 357–366.
- [7] U. Costantino, F. Marmottini, M. Sisani, T. Montanari, G. Ramis, G. Busca, M. Turco, G. Bagnasco, Cu–Zn–Al hydrotalcites as precursors of catalysts for the production of hydrogen from methanol, *Solid State Ionics* 176 (2005) 2917–2922.
- [8] R. Zhao, C. Yin, H. Zhao, C. Liu, Synthesis, characterization, and application of hydrotalcites in hydrosulfurization of FCC gasoline, *Fuel Process. Technol.* 81 (2003) 201–209.
- [9] A.E. Palomares, J.M. López-Nieto, F.J. Lázaro, A. López, A. Corma, Reactivity in the removal of SO<sub>2</sub> and NO<sub>x</sub> on Co/Mg/Al mixed oxides derived from hydrotalcites, *Appl. Catal. B* 20 (1999) 257–266.
- [10] F. Kovanda, K. Jiratova, J. Rymes, D. Kolousek, Characterization of activated Cu/Mg/Al hydrotalcites and their catalytic activity in toluene combustion, *Appl. Clay Sci.* 18 (2001) 71–80.
- [11] R. Dula, R. Janik, T. Machej, J. Stoch, R. Grabowski, E.M. Serwicka, Mn-containing catalytic materials for the total combustion of toluene: the role of Mn localisation in the structure of LDH precursor, *Catal. Today* 119 (2007) 327–331.
- [12] S. Velu, N. Shah, T.M. Jyothi, S. Sivasanker, Effect of manganese substitution on the physicochemical properties and catalytic toluene oxidation activities of Mg–Al layered double hydroxides, *Micropor. Mesopor. Mater.* 33 (1999) 61–75.
- [13] K. Everaert, J. Baeyens, Catalytic combustion of volatile organic compounds, *J. Hazard. Mater.* 109 (2004) 113–139.
- [14] J.F. Lamonier, A.B. Boutoundou, C. Gennequin, M.J. Pérez-Zurita, S. Siffert, A. Aboukais, Catalytic removal of toluene in air over CoMnAl nano-oxides synthesized by hydrotalcite route, *Catal. Lett.* 118 (2007) 165–172.
- [15] M. Zimowska, A. Michalik-Zym, R. Janik, T. Machej, J. Gurgul, R.P. Socha, J. Podobinski, E.M. Serwicka, Catalytic combustion of toluene over mixed Cu–Mn oxides, *Catal. Today* 119 (2007) 321–326.
- [16] Z. Mikulová, P. Cuba, J. Balanová, T. Rojka, F. Kovanda, K. Jiratová, Calcined Ni–Al layered double hydroxide as a catalyst for total oxidation of volatile organic compounds: effect of precursor crystallinity, *Chem. Pap.* 61 (2007) 103–109.
- [17] L.A. Palacio, J.M. Silva, F.R. Ribeiro, M.F. Ribeiro, Catalytic oxidation of volatile organic compounds with a new precursor type copper vanadate, *Catal. Today* 133–135 (2008) 502–508.
- [18] S. Kannan, V. Rives, H. Knozinger, High-temperature transformations of Cu-rich hydrotalcites, *J. Solid State Chem.* 177 (2004) 319–331.
- [19] L. Chmielarz, P. Kustrowski, A. Rafalska-Lasocha, R. Dziembaj, Influence of Cu, Co and Ni cations incorporated in brucite-type layers on thermal behaviour of hydrotalcites and reducibility of the derived mixed oxide systems, *Thermochim. Acta* 395 (2002) 225–236.
- [20] I. Melián-Cabrera, M. López-Granados, J.L.G. Fierro, Thermal decomposition of a hydrotalcite-containing Cu–Zn–Al precursor: thermal methods combined with an in situ DRIFT study, *Phys. Chem. Chem. Phys.* 4 (2002) 3122–3127.
- [21] C. Barriga, J.M. Fernández, M.A. Ulibarri, F.M. Labajos, V. Rives, Synthesis and characterization of new hydrotalcite-like compounds containing Ni(II) and Mn(III) in the hydroxide layers and of their calcination products, *J. Solid State Chem.* 124 (1996) 205–213.
- [22] F. Kovanda, T. Grygar, V. Dorničák, T. Rojka, P. Bezdička, K. Jiratová, Thermal behaviour of Cu–Mg–Mn and Ni–Mg–Mn layered double hydroxides and characterization of formed oxides, *Appl. Clay Sci.* 28 (2005) 121–136.
- [23] A.A. Mirzaei, H.R. Shaterian, M. Habibi, G.J. Hutchings, S.H. Taylor, Characterization of copper-manganese oxide catalysts: effect of precipitate ageing upon

- the structure and morphology of precursors and catalysts, *Appl. Catal. A: Gen.* 253 (2003) 499–508.
- [24] R.L. Frost, Z. Ding, W.N. Martens, T.E. Johnson, J.T. Klopogge, Molecular assembly in synthesised hydrotalcites of formula  $\text{Cu}_x\text{Zn}_{6-x}\text{Al}_2(\text{OH})_{16}(\text{CO}_3)_4\text{H}_2\text{O}$ —a vibrational spectroscopic study, *Spectrochim. Acta A* 59 (2003) 321–328.
- [25] T. López, P. Bosch, M. Asomoza, R. Gómez, E. Ramos, DTA-TGA and FTIR spectroscopies of sol-gel hydrotalcites: aluminum source effect on physicochemical properties, *Mater. Lett.* 31 (1997) 311–316.
- [26] J.T. Klopogge, R.L. Frost, Infrared emission spectroscopic study of the thermal transformation of Mg-, Ni- and Co-hydrotalcite catalysts, *Appl. Catal. A: Gen.* 184 (1999) 61–71.
- [27] M.J.L. Ginés, C.R. Apesteguía, Thermal decomposition of Cu-based hydroxycarbonate catalytic precursors for the low-temperature co-shift reaction, *J. Therm. Anal. Calorim.* 50 (1997) 745–756.
- [28] B.L. Kniep, F. Girgsdies, T. Ressler, Effect of precipitate aging on the microstructural characteristics of Cu/ZnO catalysts for methanol steam reforming, *J. Catal.* 236 (2005) 34–44.
- [29] X.R. Zhang, L.C. Wang, C.Z. Yao, Y. Cao, W.L. Dai, H.Y. He, K.N. Fan, A highly efficient Cu/ZnO/Al<sub>2</sub>O<sub>3</sub> catalyst via gel-coprecipitation of oxalate precursors for low-temperature steam reforming of methanol, *Catal. Lett.* 102 (2005) 183–190.
- [30] Y. Tan, H. Xie, H. Cui, Y. Han, B. Zhong, Modification of Cu-based methanol synthesis catalyst for dimethyl ether synthesis from syngas in slurry phase, *Catal. Today* 104 (2005) 25–29.
- [31] E.R. Stobbe, B.A. de Boer, J.W. Geus, The reduction and oxidation behaviour of manganese oxides, *Catal. Today* 47 (1999) 161–167.
- [32] O.W. Perez-Lopez, A.C. Farias, N.R. Marcilio, J.M.C. Bueno, The catalytic behavior of zinc oxide prepared from various precursors and by different methods, *Mater. Res. Bull.* 40 (2005) 2089–2099.
- [33] T. Punniyamurthy, L. Rout, Recent advances in copper-catalyzed oxidation of organic compounds, *Coord. Chem. Rev.* 252 (2008) 134–154.
- [34] S.C. Kim, W.G. Shim, Recycling the copper based spent catalyst for catalytic combustion of VOCs, *Appl. Catal. B* 79 (2008) 149–156.
- [35] W.B. Li, W.B. Chu, M. Zhuang, J. Hua, Catalytic oxidation of toluene on Mn-containing mixed oxides prepared in reverse microemulsions, *Catal. Today* 93–95 (2004) 205–209.